Characterization of Three Crystalline Forms (VIII, XI, and XII) and the Amorphous Form (V) of Delavirdine Mesylate Using ^{13}C CP/MAS NMR

Ping Gao[1,2]

Received March 18, 1997; accepted June 2, 1998

Purpose. The application of solid-state nuclear magnetic resonance (NMR) characterization of three crystalline forms (VIII, XI, XII) and the amorphous form V of delavirdine mesylate (DLV-M) is presented.
Methods. Conventional ^{13}C CP (cross-polarization)/MAS (magic angle spinning) NMR and related spectral editing methods were employed. NMR relaxation times ($T_{1\rho H}$, T_{1H}, and T_{1C}) were also measured.
Results. Distinctly different spectral features among the four solid forms were observed, indicating high sensitivity of ^{13}C NMR to the variations in solid structure. Assessment based on NMR data suggests that both anhydrous forms VIII and XI may contain one molecule per asymmetric unit. DLV may adopt a similar molecular conformation in the two forms. In contrast, form XII is found to consist of two molecules per asymmetric unit. Molecule conformation of DLV in forms VIII, XI, and XII is altered from the dominant conformer in solution. The amorphous form V may contain DLV molecules of a variety of conformations. NMR relaxation times ($T_{1\rho H}$, T_{1H}, and T_{1C}) provide valuable information about the motional characteristics in these solids. Values and the rank order of $T_{1\rho H}$, T_{1H}, and T_{1C} also reveal significant differences in local environments and the short range order among the four forms.
Conclusions. Four solid forms of DLV-M (V, VIII, XI, and XII) can be distinctly differentiated by ^{13}C CP/MAS NMR spectroscopy and their structural difference can be partially revealed without obtaining single crystal data. NMR relaxation times reveal motion dynamics and aid structural elucidation for these forms.

KEY WORDS: polymorph; pseudopolymorph; conformation; relaxation times; ^{13}C CP/MAS NMR.

INTRODUCTION

Delavirdine mesylate (DLV-M, structure shown in Figure 5) is a potent non-nucleoside reverse transcriptase inhibitor being developed for the treatment of Acquired Immune Deficiency Syndrome (AIDS) at Pharmacia and Upjohn (1). DLV-M crystallizes in a variety of different solid forms (2). Among them, forms VIII, XI and XII are crystalline while form V is an amorphous material. Forms VIII and XI are both nonhygroscopic anhydrates and form an enantiotropic pair. In contrast, form XII is a solvate and contains non-stoichiometric amounts of solvent/water (2). The crystal structures of these forms are not known due to difficulties in obtaining satisfactory crystals of appropriate size.

Probing molecular conformation involved in polymorphism has been a long-standing issue of great interest in pharmaceutical industry. This is aimed at fundamental understanding of the interplay between the inter- and intra-molecular interactions in polymorphic systems and structure-performance-property relationships for pharmaceutical application. Solid state ^{13}C NMR spectroscopy has demonstrated the capability to probe the solid materials at their molecular level. By correlating the spectral features with known structure from X-ray crystallographic studies, it has been possible to identify the influence of different structural features upon the NMR parameters (i.e., chemical shift and relaxation behavior) (3–6). These correlations can be used to deduce the molecule conformation in solid-state; this is particularly useful in instances where the crystallographic characterization of polymorphs is not available (7–15).

This study focuses on characterization of three crystalline forms (VIII, XI, XII) and the amorphous form (V) of DLV-M using solid state ^{13}C NMR. This is a natural extension of the recent work using ^{13}C CP/MAS NMR for quantitative determination of (pseudo)polymorphic mixture composition of DLV-M (16). Conventional CP/MAS NMR and related spectral editing techniques, or the non-quaternary suppression (NQS) (17) and the cross-polarization and polarization inversion (CPPI) (18), were applied for unambiguous assignments of individual resonances of these forms. Comparisons of NMR spectra of the different crystal forms provide insight into the molecule conformation and arrangement. NMR relaxation times of these forms were also measured, revealing motion characteristics of each form and significant difference in local environments.

EXPERIMENTAL METHODS AND MATERIALS

Materials

Forms V, VIII, XI and XII of DLV-M were isolated in the research laboratories of Pharmacia & Upjohn. About 200–250 mg of each form was packed into a rotor of zirconium dioxide (7 mm diameter) for CP/MAS NMR measurement.

Methods

A Bruker MSL-200 NMR spectrometer with an Oxford wide-bore (89 mm) magnet was used to perform all experiments. The static field of the superconducting magnet was 4.7T, the spectrometer operated at 50.3 MHz for ^{13}C and 200.05 MHz for ^{1}H. A doubly tuned, single-coil CP/MAS double gas bearing type probe (Bruker) was employed. The magic angle was adjusted using a KBr sample which afforded a spinning angle of 54.7° ± 0.3° (19). The samples were usually spun at 4.5 kHz (± 2 Hz). The Hartmann-Hahn match was established at the center-band match condition using adamantane.

Proton spin-lattice relaxation time in the laboratory frame (T_{1H}), proton spin-lattice relaxation time in the rotating frame ($T_{1\rho H}$), the cross-polarization transfer rate constant (T_{CH}) and carbon-13 spin-lattice relaxation time in the laboratory frame (T_{1C}) of each form were measured through CP/MAS NMR related pulse sequences via the detection of carbon signals (20). An appropriate phase-cycling scheme with ^{1}H flipback pulse was employed (20). The acquisition parameters were: spectral width: 20 kHz; contact time: 2 ms; repetition time: 5 s; and 90° ^{1}H pulse width: 3.5 μs. NQS spectra of the samples were

[1] Pharmaceutical Development, Pharmacia & Upjohn, 301 Henrietta Street, Kalamazoo, Michigan 49001.
[2] To whom correspondence should be addressed. (e-mail: ping.gao@am.pnu.com)

0724-8741/98/0900-1425$15.00/0

obtained with a dipolar dephasing time (t_{DD}) around 30 to 50 μs. CPPI spectra were obtained with an equal polarization inversion time of t_{PI1} and t_{PI2} between 40 and 60 μs (18). ^{13}C chemical shifts were calibrated indirectly to the higher field adamantane peak (29.5 ppm relative to tetramethylsilane). The chemical shifts listed in Table 1 are accurate to ± 0.3 ppm, but within one spectrum the relative shifts are more accurate (~0.1 ppm). The editorial treatments (linear combination) of experimental spectra were performed on the ASPECT 3000 spectrometer computer.

RESULTS AND DISCUSSION

DLV-M contains 23 carbons (Fig. 5 and Table 1); methyl, methylene, methine and quaternary carbons are simultaneously present in the molecule. The chemical shifts of the ^{13}C CP/MAS NMR spectra of the solid forms provide diagnostic information regarding the local environment of individual carbons. Therefore, correct assignments of these resonances are critical in interpretation of the spectral features. In this work, these assignments are based on the combination of three approaches. First, the non-quaternary suppressing (NQS) experiment displays resonances only arising from the quaternary and methyl carbons (17). Secondly, the CPPI experiment further differentiates the methine from the methylene resonances (18). Thirdly, the chemical shifts of the CP/MAS NMR spectra are compared to solution NMR for assignments.

Form XI

Figure 1A shows the conventional ^{13}C CP/MAS NMR spectrum of form XI (few spinning side bands marked with asterisk). The NQS spectrum of form XI is shown in Figure 1B. Methyl resonances are readily separated from the quaternary resonances based on their chemical shifts. The resonances at 20.2, 23.7, 38.2 and 44.7 ppm are assigned to four methyl carbons (C9′, C9′, C9, and C15). Note that the DLV-M molecule contains two chemically equivalent methyls (C9′) and they are magnetically nonequivalent in form XI. This observation indicates a high sensitivity of methyl group towards different environments. Resonances between 120 and 170 ppm are associated with seven quaternary carbons; most of them appear as doublets with an asymmetric intensity distribution: a higher intensity peak located upfield and accompanied by a lower intensity peak downfield. This is characteristic of incompletely depressed ^{14}N-^{13}C dipolar coupling (10,15). The doublets observed at 128.6/131.8, 134.6/136.0, 143.1/145.5 and 161.0/163.0 ppm (Fig. 1B) are assigned to C2 and C7a of the indole ring, C2′ of the pyridine and the carbonyl carbon C10, respectively. The splitting resonances of C3′ of the pyridine are shown at 139.0 and 140.0 ppm while the intense singlet at 127.3 ppm is assigned to C3a and C5 together.

Figure 1C shows the CPPI spectrum of form XI. The spectrum consists of intense positive signals of the quaternary and methyl carbons and *negative* signals of the methine and methylene carbons (18). In order to unambiguously separate the methine from the methylene resonances, editorial treatment was necessary. The CPPI spectrum was multiplied by an appropriate factor (1.3) and added to its conventional CP/MAS NMR spectrum (Fig. 1A) to cancel the methylenes' intensities (e.g., 50.0 ppm) (18). This results in a spectrum (not shown) that enhances the methine resonances with the presence of quaternary and methyl resonances. This spectrum was further simpli-

Table 1. Chemical Shifts of DLV-M Observed in Solid Forms XI, VIII, XII, V, and in Solution (DMSO-d_6)

			Form XI		Form VIII		Form XII		Form V	
Carbon #	Functionality	Solution	δ(^{13}C)	Δ	δ(^{13}C)	Δ	δ(^{13}C)	Δ	δ(^{13}C)	Δ
9′	CH_3	21.7	20.2	−1.5	17.3	−4.4	19.1	−2.6	22.2	0.5
9′	CH_3	21.7	23.7	2.0	23.9	2.2	21.2/22.2	−0.5/0.5	22.2	0.5
8′	N-CH	43.4	44.2	0.8	45.2	0.9	41.6/44.4/48.4	−0.4	—[a]	—[a]
2′	N-C-N	146.9	143.1/145.5	−2.6	146.4	−0.5	142.2	−4.6	144.3	−2.6
3′	N-C	137.1	139.0/140.0	2.4	140.6	3.6	136.2	−0.9	137.8	0.7
4′	CH	127.0	127.3	0.3	124.7	−2.3	124.3	−2.7	122.3	−4.7
5′	CH	120.5	124.2	3.7	123.4	2.9	121.6	1.1	122.3	1.8
6′	N-CH	120.9	127.3	6.4	124.7	3.8	122.6	1.7	122.3	1.4
11 (13)	$N-CH_2$	48.0	48.6	0.6	49.6	1.6	48.4	0.4	47.3	−0.7
13 (11)	$N-CH_2$	48.0	50.0	2.0	49.6	1.6	48.4	0.4	47.3	−0.7
12 (14)	$N-CH_2$	44.0	41.7	−2.3	44.2	0.2	44.4	0.4	44.5	0.5
14 (12)	$N-CH_2$	44.0	45.7	1.7	44.2	0.2	44.4	0.4	44.5	0.5
10	N-C=O	161.8	161.0/163.0	−0.2	158.6/160.3	−2.4	161.0	−0.8	162.3	0.5
2	N-C	130.6	128.6/131.8	−0.4	131.0	0.4	129.7	−0.9	130.2	−0.4
3	CH	104.3	106.4	2.1	106.0	1.7	108.3	4.0	106.2	1.9
3a	C	127.0	127.3	0.3	129.4	2.4	127.0	0	127.3	0.3
4	CH	114.4	112.5	−1.9	122.1	7.7	119.0	4.6	113.0	−1.4
5	N-C	130.3	127.3	−3.0	129.4	−0.9	127.0	−3.3	127.3	−3.0
6	CH	119.7	115.8	−3.9	122.1	2.4	120.8	1.1	122.3	2.6
7	CH	112.6	112.5	0.1	113.2	0.6	115.6	3.0	113.0	0.4
7a	N-C	133.5	134.6/136.0	1.8	135.2/136.4	2.3	136.2	−2.7	134.8	1.3
9	CH_3-SO_2NH	38.3	38.2	−0.1	38.4	0.1	36.8	−1.5	40.0	1.7
15	CH_3-SO_2OH	39.7	44.7	5.0	40.4	0.7	37.8	−1.9	49.4	9.7

[a] Unable to resolve.

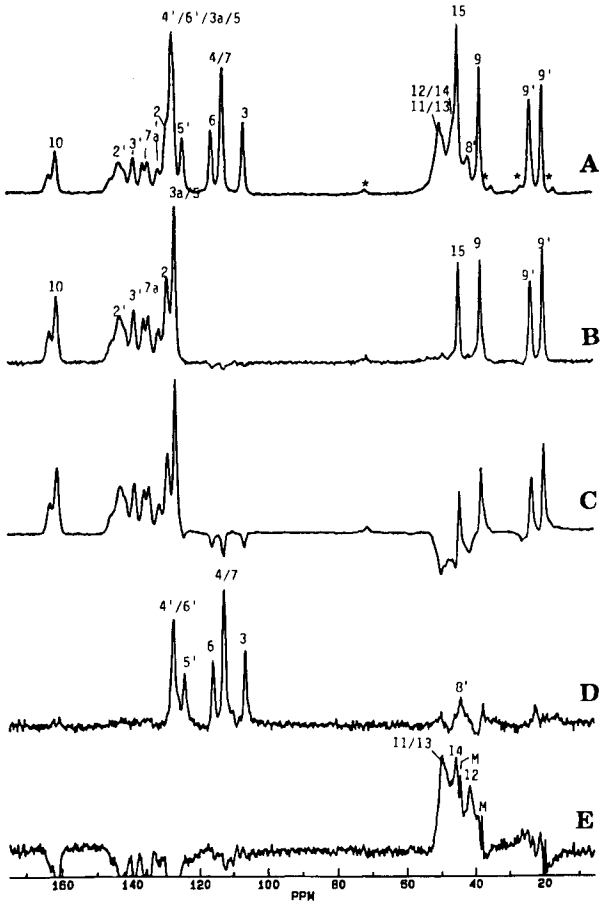

Fig. 1. ^{13}C spectra of form XI of DLV-M: (A) the conventional CP/MAS NMR spectrum (number of scans, ns = 640); (B) the NQS spectrum (ns = 640) with t_{DD} = 45 μs; (C) the CPPI spectrum (ns = 1600) with t_{PI} = 30 μs; (D) the CH subspectrum; and (E) the CH_2 subspectrum; M denotes the residual methyl resonance indicating the imperfection resulting from the spectral editorial treatment.

fied by removing the quaternary and methyl resonances through subtracting the NQS spectrum (Fig. 1B). The resulting methine subspectrum is shown in Figure 1D (some weak methyl signals are still observable because of imperfect cancellation). The weak, broad resonance at 44.2 ppm is assigned to C8′, consistent with its chemical shift in solution (21). This weak resonance is significantly buried by surrounding intense methyl and methylene resonances and would be difficult to identify otherwise. Furthermore, this subspectrum clearly reveals that the intense resonance observed at 127.3 ppm (Fig. 1D) is classified as the methine type, which is overlapped with the quaternary carbon resonances (C3a and C5) at the *same* position (Fig. 1B). It would be *impossible* to reveal its dual identities without applying the spectral editing techniques. Resonances at 112.5 and 127.3 ppm both represent two aromatic methine carbons (C4 and C7 of the indole ring; C4′ and C6′ of the pyridine ring). The singlet resonances at 106.4, 115.8, and 124.2 ppm are assigned to C3, C6, and C5′. Therefore, six ^{13}C resonances in Figure 1D account for all eight methine carbons in DLV-M.

Editorial treatment was also performed to obtain a $^{13}CH_2$ subspectrum. The CPPI spectrum of DLV-M was multiplied by an appropriate factor (1.3) and added to its standard CP/MAS NMR spectrum (Fig. 1A) to cancel the methines' intensities. Then, the spectrum obtained (not shown) was phase reversed showing methylene resonances with the presence of negative intensities of quaternary and methyl signals. The spectrum was further simplified by cancelling the quaternary and methyl resonances through addition to the NQS spectrum (Fig. 1B). Figure 1E is the resulting subspectrum. Four resonances significantly overlap each other with splitting characteristics due to incompletely suppressed ^{13}C-^{14}N dipolar coupling. The resonances at 41.7 and 45.7 ppm, and a broad doublet at 48.6/50.0 ppm are tentatively assigned to the four methylene carbons of the piperazine ring (C12/C14, C11/C13, interchangeable). The chemical shifts and assignments of form XI are summarized in Table 1. As the ^{13}C spectrum shows sharp resonances without indication of crystallographic splitting, form XI may contain one molecule per asymmetric unit.

Form VIII

Figure 2A shows the conventional ^{13}C CP/MAS NMR spectra of form VIII and Figure 2B shows the NQS spectrum. Resonances observed at 17.3, 23.9, 38.4 and 40.4 ppm are assigned to methyls of C9′, C9′, C9, and C15. Note that the two chemically equivalent methyls (C9′) are also magnetically nonequivalent. Similar to form XI, resonances between 120 and

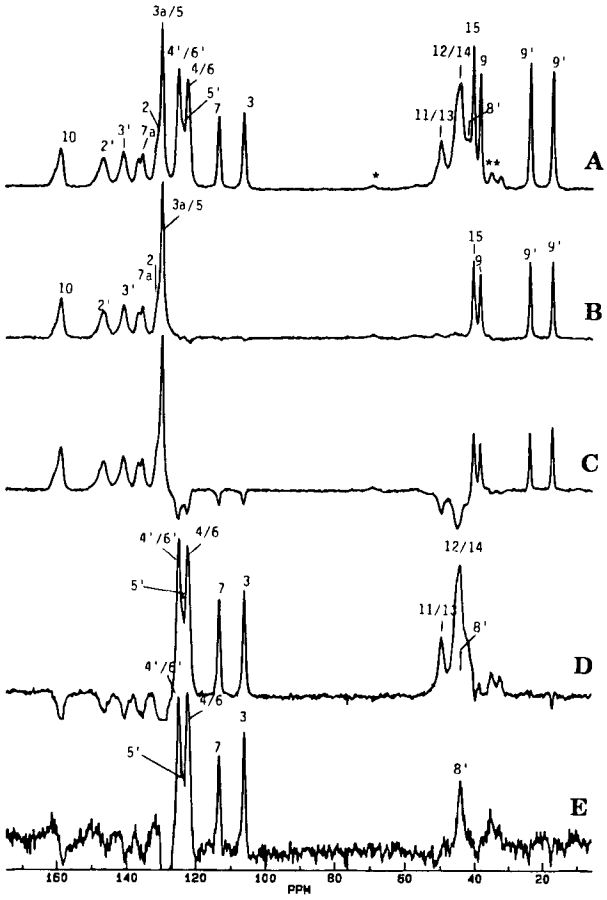

Fig. 2. ^{13}C spectra of form VIII of DLV-M: (A) the conventional CP/MAS NMR Spectrum (ns = 640); (B) the NQS Spectrum (ns = 640) with t_{DD} = 45 μs; (C) the CPPI spectrum (ns = 640) with t_{PI} = 30 μs; (D) the (CH + CH_2) subspectrum; and (E) the CH subspectrum.

170 ppm exhibit doublet features with an asymmetric intensity distribution, indicative of the incompletely depressed ^{14}N-^{13}C coupling. The doublets observed at 135.2/136.4 and 158.6/160.3 ppm (Fig. 2B) are assigned to C7a and C10. Broad resonances at 131.0 (appears as a shoulder to the intense 129.4 ppm resonance), 140.6, and 146.4 ppm are assigned to C2 of the indole ring and C3′ and C2′ of the pyridine ring. The intense singlet at 129.5 ppm is assigned to C3a and C5 together.

Figure 2C shows the CPPI spectrum of form VIII; the subspectrum (Fig. 2D) that displays the methine and methylene signals is obtained by subtracting the NQS spectrum (Fig. 2B) from the standard CP/MAS NMR spectrum (Fig. 2A). A subspectrum (Fig. 2E) that only displays the methine resonances was obtained in the same manner as described above for form XI. Similar to form XI, the *hidden*, broad resonance at 44.2 ppm with splitting characteristics is assigned to C8′ while resonances at 122.1 and 124.7 ppm both represent two methine groups (C4 and C6 of indole ring; C4′ and C6′ of pyridine ring). The singlet resonances at 106.0, 113.2, and 123.4 ppm (shown between 122.1 and 124.7 ppm resonances) are assigned to C3, C7 and C5′.

Similar to form XI, broad resonances in the region of 30 to 50 ppm (Fig. 2D) are dominated by the methylene carbons. The broad resonances at 44.2 and 49.6 ppm are poorly resolved and assigned to C12/C14 and C11/C13 (interchangeable). Chemical shifts and assignments of form VIII are also summarized in Table 1. Exhibiting sharp resonances without indication of crystallographic splitting, form VIII may contain one molecule per asymmetric unit.

Form XII

Figure 3A shows the conventional ^{13}C CP/MAS NMR spectra of form XII with complex features. Figure 3B shows its NQS spectrum; the resonance at 19.2 ppm is assigned to one of the two C9′ methyls while the doublet of equal intensity at 21.2/22.2 ppm is assigned to the other C9′. This doublet indicates two magnetically nonequivalent methyls of the isopropyl group, commonly referred as crystallographic splitting (6). The other methyl resonances at 36.8 ppm and 37.9 ppm are assigned to C9 and C15. Resonances between 120 and 170 ppm are significantly broader compared to forms XI and VIII, losing fine features. Resonances at 129.7, 142.3 and 161.0 ppm (Fig. 3B) are assigned to C2, C2′, and C10; the broad resonance at 136.2 ppm is assigned to two quaternary carbons (C7a and C3′). The intense singlet at 129.5 ppm is assigned to C3a and C5 together.

Figure 3C shows the CPPI spectrum of form XII. The subspectrum that displays the methine and methylene signals was obtained in the same manner described above and is shown in Figure 3D; a subspectrum that only displays the methine resonances is shown in Figure 3E. Similar to forms XI and VIII, the hidden resonances appear as a triplet at 41.6, 44.4 and 48.4 ppm, and are assigned to C8′ only. The triplet feature is attributed to the overlap of two doublets; each doublet is caused by incompletely suppressed ^{14}N-^{13}C dipolar coupling. This is in good agreement with the doublet feature of the methyl group (one C9′) discussed above; these observations together suggest two molecules of the *same* conformation per asymmetric unit in form XII. Supporting this argument, the relatively broad resonances observed in this form are primarily due to

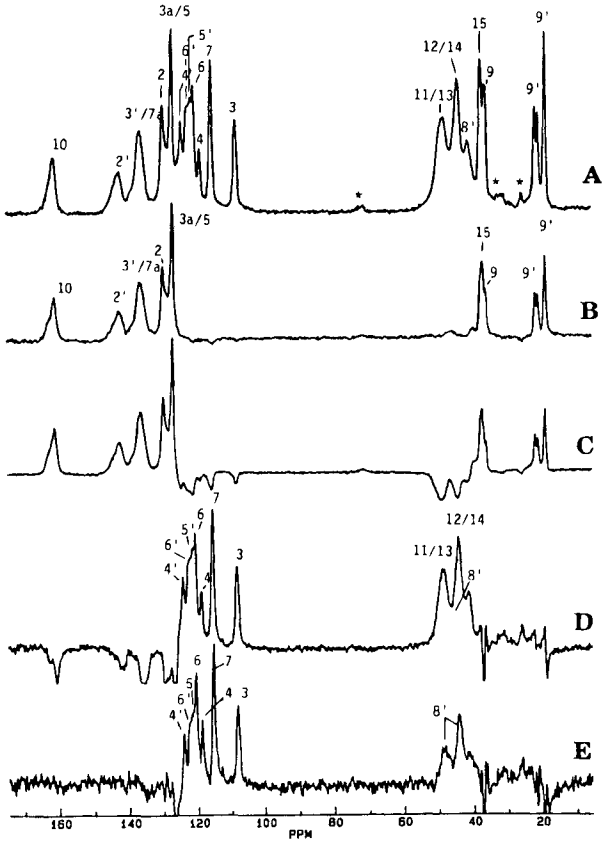

Fig. 3. ^{13}C spectra of form XII of DLV-M: (A) the conventional CP/MAS NMR spectrum (ns = 640); (B) the NQS spectrum (ns = 640) with t_{DD} = 45 μs; (C) the CPPI spectrum (ns = 1600) with t_{PI} = 30 μs; (D) the (CH + CH_2) subspectrum; and (E) the CH subspectrum.

overlapping resonances of the two molecules. Broad, singlet resonances at 108.3, 115.6 and 119.0 ppm are assigned to quaternary carbons C3, C7 and C4. The overlapping resonances at 120.8, 121.6 and 122.6 ppm and the singlet resonance at 124.3 ppm are assigned to C6 of the indole ring and C5′, C6′ and C4′ of the pyridine ring, respectively (Fig. 3E).

Compared to Figure 3E, the broad resonances in the 30–50 ppm region of Figure 3D are dominated by the methylene resonances which significantly overlap with the methine resonance (C8′) identified above. Due to incompletely suppressed ^{13}C-^{14}N coupling and crystallographic splitting, the poorly-resolved resonances at 44.4 and 48.4 ppm are tentatively assigned to C12/C14 and C11/C13. The chemical shifts and assignments of form XII are also summarized in Table 1.

Form V

Form V is the amorphous form of DLV-M (2). Its conventional ^{13}C CP/MAS NMR and NQS spectra are shown in Figure 4A and 4B. As expected, very broad resonances are observed with linewidths at the half height about 250 Hz or larger. (In contrast, the crystalline forms exhibit narrow signals; the linewidth is typically less than 40 Hz). The resonances observed at 22.2, 40.0, and 49.4 ppm are assigned to C9′/C9′, C9, and C15. The amorphous form shows that the two chemically equivalent methyls (C9′) appear as one very broad resonance in

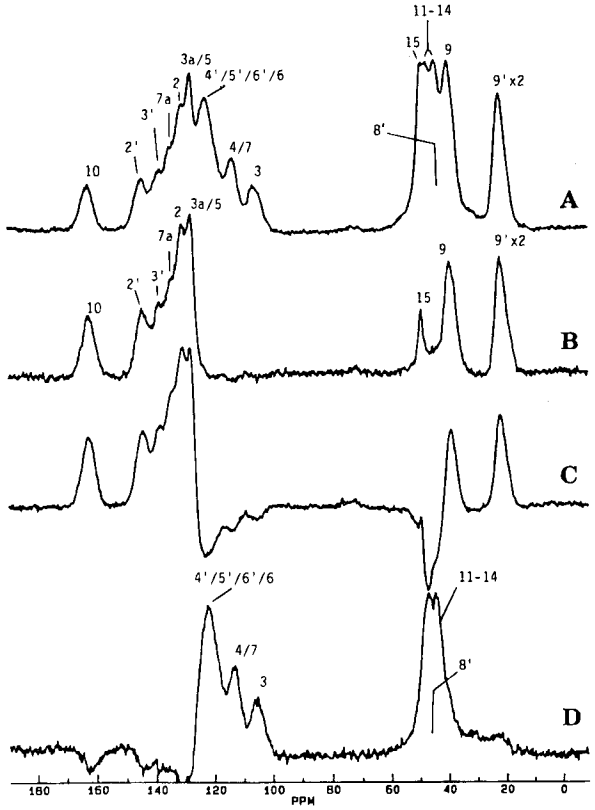

Fig. 4. ^{13}C spectra of form V of DLV-M: (A) the conventional CP/MAS NMR spectrum (ns = 640); (B) the NQS spectrum (ns = 640) with t_{DD} = 45 μs; (C) the CPPI spectrum (ns = 1600) with t_{PI} = 30μs; and (D) the (CH + CH_2) subspectrum.

contrast to the crystalline forms. This is presumably attributed to the occupation of the methyl carbons in a variety of sites and diminishment of the fine structure. Resonances between 120 and 170 ppm are broad and tentatively assigned to seven quaternary carbons as given in Table 1. Figure 4C shows the CPPI spectrum of form V. Then, the subspectrum that displays the methine and methylene signals was obtained similarly and is shown in Figure 4D. Similar to other forms discussed above, broad resonances in the region of 30–50 ppm (Fig. 4D) are dominated by the methylene resonances. It is difficult to reveal the hidden methine resonance (C8′). Broad resonances at 106.2, 113.0 and 122.3 ppm are attributed to six methine carbons and tentative assignments are given in Table 1.

Molecule Arrangement in the Solid Forms

Previous investigations of isotropic chemical shifts in solids reveal that the chemical shielding parameters are primarily a property of the molecule itself and does not change substantially as the molecule solidifies from the liquid state. Many carbon resonances show essentially the same positions within few ppm due to medium effect (i.e., desolvation) (except where changes of bonding occur such as the formation of hydrogen-bonding or structural transformation in tautomeric equilibria) (7,9,10,12,15). Thus, the rank order of chemical shifts and well-established relationships of these chemical shifts with structural features derived from liquid-state can be used with caution in interpreting and assigning corresponding signals from solids, at least as a first approximation.

Although the isotropic chemical shifts obtained from solids under MAS are generally close to those measured in solution, an inherently different facet of such experiments on solids is the absence of dynamic averaging (which occurs readily in solution). Hence, the molecular conformations are "*locked*" in position due to "freezing" of free rotation of bulky substituents. Both intramolecular (conformational) and intermolecular (crystal packing) interactions are known to play important roles in determining the magnetic environment of individual nuclei in solids (9,10–12,15). Thus, chemical shift is sensitive to changes in the immediate environment of the nucleus and provides the most diagnostic information.

Knowing all ^{13}C resonances' assignment, it is of great interest to compare the chemical shift variation among the four DLV-M forms in order to reveal their structural difference in terms of conformation and packing effects. Note that the chemical shift of the methyl groups varies among these three crystalline forms. Form XI shows methyl resonances at 20.2, 23.7, 38.2, and 44.7 ppm, form VIII shows methyl resonances at 17.3, 23.9, 38.4, and 40.4 ppm and form XII shows the counterparts at 19.1, 21.2/22.2 (doublet), 36.8 and 37.8 ppm (Table 1). The nonequivalence of the two chemically equivalent isopropyl methyl groups (C9′) is obvious in *all* three crystalline forms whereas a single resonance (21.7 ppm) is observed in solution as a result of isotropic motion averaging. This indicates that the two isopropyl methyls are located in different crystallographic sites with chemical shifts varying from +2.2 to −4.4 ppm from the isotropic solution value (Table 1). The methyls from the terminating sulfonamido group (C9) and the sulfonate ion (C15) also exhibit significant deviations in chemical shifts (−1.9 to +5.0 ppm from the solution value, Table 1) among the crystalline forms VIII, XI, and XII.

Previous studies reveal that the packing effects are usually insignificant and its influence upon the chemical shifts is no greater than 2–3 ppm (9,12). Therefore, packing effects of this magnitude alone are not sufficient to explain the observed difference in the ^{13}C chemical shifts of these methyl carbons among the solid forms. Difference in intramolecular geometries, or conformational changes, are presumably the main cause of the large variation of chemical shifts observed. The chemical shift of methyl carbons in organic solids is known for its sensitivity towards crystallographic site (10–12). Indeed, the great variation of the chemical shift of all these methyl groups among the three crystalline forms indicates variations in crystallographic sites of the isopropyl and terminating sulfonamido side chains as well as the sulfonate ions.

Figure 5 shows the ^{13}C spectra of forms VIII and XI with all resonances labelled. The resonances of the isopropyl side chain (C9′ at 23.9 ppm, C8′), the piperazine ring (C11–C14) and the terminating sulfonamido side chain (C9) overlap between forms VIII and XI with a small difference of chemical shift around 0.5–1 ppm (Table 1). The chemical shifts of C2, C3, C3a, C7a, C5 and C7 on the indole ring are also similar in the two forms except for C4 and C6. However, substantial differences of chemical shifts are apparent between the two pyridine rings (C2′–C6′). Since the two forms may both contain one molecule per asymmetric unit, these observations together suggest a similar skeleton conformation of DLV-M in forms

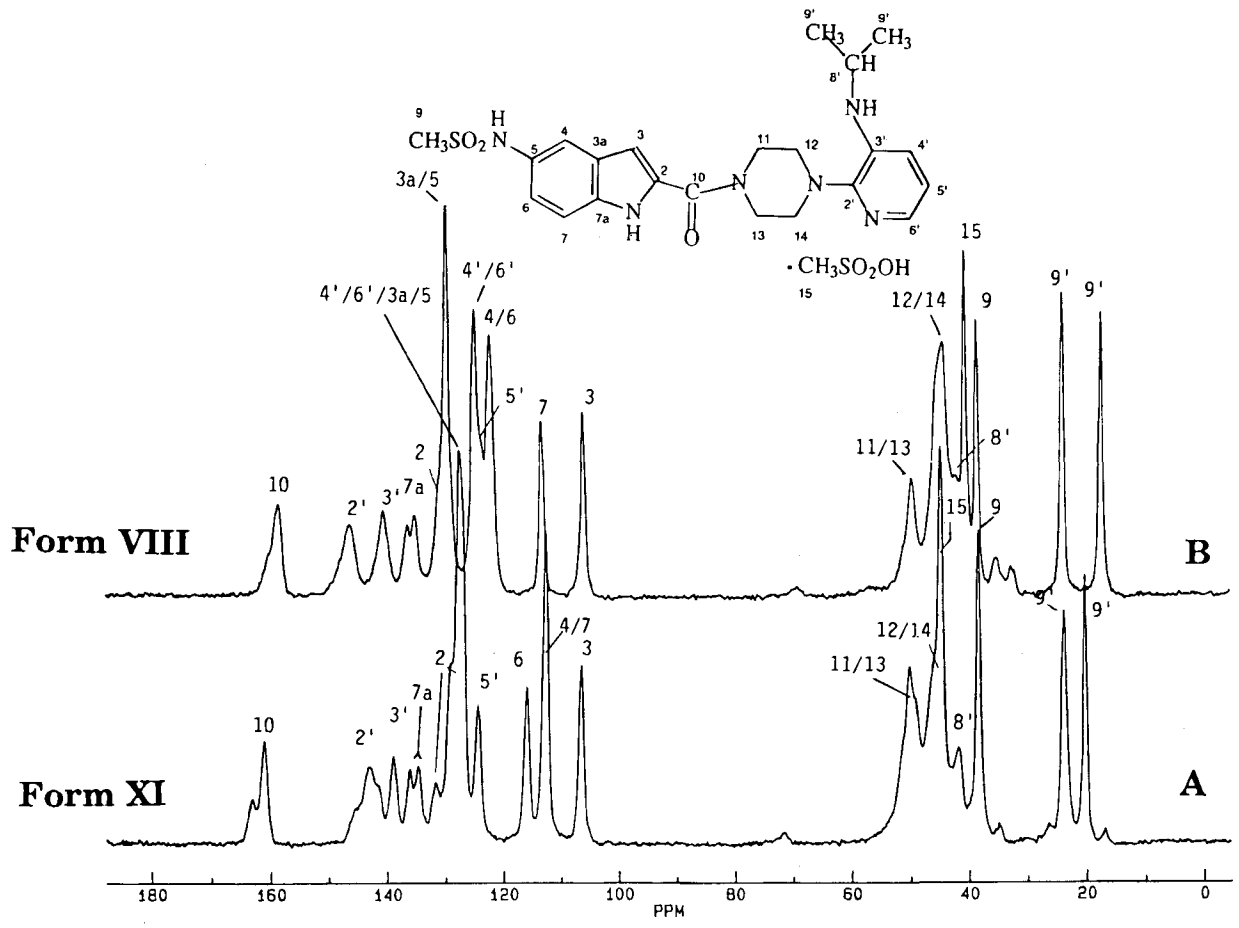

Fig. 5. ^{13}C CP/MAS NMR spectra of forms XI (A) and VIII (B) of DLV-M with resonances assignment.

VIII and XI with some variations in the local environment of the pyridine ring and part of the indole ring (C4, C6).

In contrast to forms XI and VIII, form XII consists of two molecules per asymmetric unit; the crystallographic splitting and the broadness of resonances are primarily attributed to very small differences between the two molecules of the same conformation. Since form XII is an *undefined solvate* that gradually desolvates and contains little amount of methanol/acetone and approximately 6% water at the time of analysis (2). Its large deviation of chemical shifts compared to forms VIII and XI may partially arise from the loose incorporation of guest solvent molecules in the lattice.

Differences of the chemical shift between each solid form and the solution value ($\Delta = \delta$ (solid) $- \delta$ (solution)) are also given in Table 1. Solution NMR spectra yield chemical shifts which are either characteristic of the magnetic environment for individual nuclei in the preferential conformation, or the "average" chemical shifts of several possible conformations resulting in rapid equilibrium with one another. As summarized above, solvation or desolvation usually slightly affects the resonance within few ppm. Significant differences of the chemical shift of each functional group (i.e, isopropyl side chain, pyridine ring, piperazine ring, indole ring and terminating sulfonamido side chain) between the solution state and three solid forms are apparent. Therefore, it suggests that none of the conformations adopted by the three crystal forms dominates in solution. This implies that significant intra- and/or inter-molecular interactions occur and the molecular conformation changes when the molecules crystallize.

The amorphous form V exhibits a general broadness of the ^{13}C resonances. This is attributed to the co-existence of many different conformations which give rise to a dispersion of chemical shifts for each resonance. $T_{1\rho H}$ and T_{1C} relaxation times measurement further reveals a disordered feature of form V (vide infra).

NMR Relaxation Behaviors

NMR relaxation times were measured in order to reveal motion dynamics and aid structural elucidation for these forms. Three relaxation times (T_{1H}, $T_{1\rho H}$, and T_{1C}) were measured for each system and discussed below.

$T_{1\rho H}$ Relaxation Times

The proton spin-lattice relaxation time in the rotating frame, $T_{1\rho H}$, is presumably sensitive to the intermolecular interaction and may vary with the phase structure (i.e., degree of order, crystallinity) (22). $T_{1\rho H}$ values of each form were obtained at room temperature by recording ^{13}C resonance intensities as a function of variable spin-lock time and through an exponential fit (16). Essentially a single $T_{1\rho H}$ (with a standard deviation of 10–20%) is observed in all forms examined as expected due to efficient proton spin diffusion.

Table 2. Average T_{1H} and $T_{1\rho H}$ Values Observed from the DLV-M Forms Examined

	R_t	T_{1H} (Avg.)(s)	$T_{1\rho H}$ (Avg.)(ms)
Form VIII	2.7	1.87 ± 0.04	234 ± 25
Form XI	3.5	1.34 ± 0.03	448 ± 80
Form XII	3.7	1.03 ± 0.08	27.5 ± 2.8
Form V	2.5	1.44 ± 0.10	8.0 ± 1.2

The average $T_{1\rho H}$ values of these forms are reported in Table 2. Note that form XI exhibits a $T_{1\rho H}$ value around 450 ms and form VIII exhibits a $T_{1\rho H}$ of 230 ms. In contrast, $T_{1\rho H}$s of forms XII (27 ms) and V (9 ms) are approximately one to two orders of magnitude shorter than the two highly crystalline forms. A rank order of $T_{1\rho H}$ is observed:

$$T_{1\rho H}\,(XI) > T_{1\rho H}\,(VIII) >> T_{1\rho H}\,(XII) > T_{1\rho H}\,(V)$$

Since the proton spin diffusion in solid-state is facilitated presumably through the intermolecular interactions which is largely dependent upon the proximity of the neighboring hydrogen atoms and the local intermolecular interaction, reduction of $T_{1\rho H}$ from XI to V is indicative of a decrease in short range order (a dimension typically less than 50–100 Å[3]). This is also consistent with the long range order revealed by XRD results (2). Compared to highly crystalline forms XI and VIII, form XII shows a poorer short range order, presumably due to loose incorporation of solvent molecules in the lattice and/or partial desolvation (2). The very short $T_{1\rho H}$ of form V suggests a disordered state which is attributed to poor molecule packing resulting from the coexistence of multiple conformations. These results indicate a very high sensitivity of $T_{1\rho H}$ towards the short range order in solid.

T_{1C} Relaxation Times

One of the principal advantages of T_{1C} measurement versus T_{1H} and $T_{1\rho H}$ measurements is that the relaxation time of *individual* carbons can be measured and these T_{1C}s, therefore, may provide specific information with respect to the local motion (i.e., methyl rotation, ring rotation, etc.). T_{1C} values of individual resonances in each form were measured at room temperature and are reported in Table 3. In general, most of the ^{13}C resonances' intensity of all four forms in this study can be approximately fit to a single exponential function to extract T_{1C} values without complexities.

Note that *all* methyl carbons (except for C15 of form XII) generally exhibit very short T_{1C} values compared to the other types of carbon nuclei in each form. It has been found that, in organic solids of small molecular size, the rotation of methyl groups around its C_3 axis provides the main source of the T_{1C} relaxation given that no other protonic motion is available (23). Thus, the rapid internal rotation of the methyl group modulates the ^{13}C-^{1}H (methyl proton) dipolar interaction. The motional difference among C9′ methyls are qualitatively manifested by the difference in T_{1C} values of the three *crystalline* forms (Table 3). This is in good agreement with the work by Grant et al. which pointed out that the methyl groups exhibit a wide range of rotational activities depending on the structural environment (10–12).

Table 3. T_{1C} Values Observed from the DLV-M Forms Examined

Carbon #	Form XI	Form VIII	Form XII	Form V
C9′	1	3	1	1
C9′	0.5	2.5	0.6	1
C8′	125	—[a]	33	—[a]
C9	2	0.5	1	2.2
C15	7	7	24	—
C2′	200	90	125	—
C3′	260	85	100	—
C4′	165	60	65	48
C5′	220	—	65	48
C6′	165	60	66	48
C11	150	50	33	33
C12	140	40	33	33
C13	150	50	33	33
C14	140	40	33	33
C10	190	93	125	95
C7a	180	70	109	—
C3	130	80	60	45
C3a	150	90	90	45
C4	150	60	—[a]	45
C2	—	—	90	—
C6	160	60	65	—
C7	150	60	40	45
C5	150	90	90	45

[a] Not observable.

These results presumably suggest that the motions of individual carbons or groups are profoundly dependent on the intermolecular contacts between sterically crowded molecules in the lattice. Since DLV-M is a salt, it contains methylsulfonate ions. Its crystallographic site in the crystal lattice can only be probed through its methyl group in CP/MAS NMR experiments. T_{1C} values of C15 are found to be approximately 7 s in both forms VIII and XI. This is consistent with the previous assessment that C15 experiences a comparable local environment in these two forms. This may also imply a similarity in crystal packing involving methylsulfonate ions although their chemical shifts are 4.1 ppm apart. In contrast, a significantly longer T_{1C} (24 s) of C15 observed in form XII than forms VIII and XI suggests that this methyl group may experience unusually high degree of motional freedom. This is probably associated with a different arrangement of methylsulfonate ions in the lattice, leading to a less crowded environment and exerting less steric restriction on methyl rotation. Another related possibility is that such arrangement may reduce the electrostatic interaction between negatively charged sulfonate ions and protonated positive centers of DLV molecules and, therefore, reduce the barrier for methyl rotation.

Significantly longer T_{1C}s are observed for the quaternary (C2′, C3′, C10, C2, C5′ etc.) carbons compared to the methylene and methine carbons in each form; this indicates the predominant dipolar relaxation mechanism through protons on neighboring protonated carbons. Similar to the $T_{1\rho H}$ data, the rank order of T_{1C} of *non-methyl* carbons among these forms is generally observed (Table 3):

[3] This estimation is based on spin diffusion kinetics given in Ref. 22 using the $T_{1\rho H}$ values obtained in this work.

$$T_{1C}\ (XI) > T_{1C}\ (VIII) \sim T_{1C}\ (XII) > T_{1C}\ (V).$$

Although detailed motion analysis related to T_{1C} for these forms is impossible, the rank order of T_{1C} among the four forms is in reasonable agreement with the $T_{1\rho H}$ rank order. Relatively shorter T_{1C}s of form V compared to those crystalline forms suggest more significant molecule motion activities, implying a disordered state. Conversely, the very long T_{1C}s of form XI are indicative of a more rigid, well organized crystal lattice (24).

T_{1H} Relaxation Times

The proton spin-lattice relaxation in the laboratory frame, T_{1H}, was also measured. A single T_{1H} value (standard deviation: ± 5%) of each form was always observed and is expected due to fast proton spin diffusion. T_{1H} values of the four forms (Table 2) show the rank order below:

$$T_{1H}\ (XII) < T_{1H}\ (XI) < T_{1H}\ (V) < T_{1H}\ (VIII)$$

Note that this trend is *inconsistent* with the rank order for $T_{1\rho H}$ and T_{1C}.

As discussed above, methyl carbons show shorter T_{1C}s than do methine and methylene carbons of the rigid molecular skeleton. This is primarily due to the methyl group rotation which is usually faster than other molecular motions. T_{1H} is known to be dominated by the internal rotation of the methyl group through proton spin diffusion (10–12,22,24). For a homogeneous organic solid, T_{1H} is essentially determined by the methyl proton relaxation (24). For DLV molecules, three methyl groups (C9′x2, C9) are presumably the relaxation-originating protons responsible for the overall proton relaxation process. By definition, the relaxation rate constant, R_i, of each nuclei is a reciprocal of its relaxation time, T_i,

$$R_i = 1/T_i \qquad (1)$$

The overall spin-lattice relaxation rate constant, R_t, can be approximately expressed as a summation of the corresponding rate constants which contribute to the process,

$$R_t = \Sigma R_i = \Sigma\ 1/T_i \qquad (2)$$

Considering that the proton relaxation of each methyl group is related to its motion activity (manifested by its T_{1C}) and averaged by fast proton spin diffusion, the relative values of the overall *proton* spin-lattice relaxation rate constant, R_t, for all four forms can be correlated to the T_{1C} of the three methyl groups (Table 3) using Eq. (2) and are reported in Table 2. Thus, the trend of T_{1H} for the three crystalline forms can be *qualitatively* interpreted based upon their difference of R_t. Form XII shows the shortest T_{1H} (1.03 s) and the largest R_t; this is attributed to the combination of three slower rotational methyls (shorter T_{1C}s: 1 s, 0.6 s, 1 s, Table 3). This implies that a less mobile methyl group experiences a stronger ^1H-^1H coupling and, therefore, leads to a more efficient relaxation process. Conversely, form VIII shows the longest T_{1H} (1.87 s) and a smaller R_t due to the combination of three faster rotational methyls (T_{1C}: 3 s, 2.5 s, 0.5 s). The relative order of T_{1H} of form XI with respect to forms XII and VIII can also be explained (Table 2). However, form V shows the smallest R_t among the four forms and this is inconsistent with the prediction using this rationale. A plausible explanation is that a variety of motion activities in the *amorphous* form V contribute significantly to the T_{1H} process and the oversimplified model fails to take them into account.

CONCLUSIONS

From a methodology point of view, the present study illustrates some of the limitations as well as strengths of solid state NMR for probing molecule conformation in organic crystals, especially in cases of polymorphism. Solid state NMR techniques do not provide independent determinations of molecular conformation. They are usually incapable of providing absolute configuration that is available from single crystal data (i.e., space group, cell dimension, geometric arrangement of atoms). However, when it is appropriately applied, it may offer a rapid assessment of some key crystallographic features (e.g., the number of molecules per asymmetric unit, long range order) and relative difference in conformation between the solution and solid states or among crystalline forms. Further, it may reveal the specificity of a local environment. Such information can be valuable when single crystal data are not available or the understanding of the physicochemical and/or biological activity associated with these crystalline forms is desired. Consequently, characterization of these crystalline forms may shed light on selection and optimization of the solid forms of the active substance in pharmaceutical application.

ACKNOWLEDGMENTS

The author would like to thank Michael Bergren for preparing the DLV-M form V; Ad Bax, Michael Bergren, and one of the reviewer for enlightening discussions and thorough criticism on the manuscript.

REFERENCES

1. I. W. Althaus, J. J. Chou, A. J. Gonzales, M. R. Deibel, K-C. Chou, F. J. Kezdy, D. L. Romero, R. C. Thomas, P. A. Aristoff, W. G. Tarpley, and F. Reusser. Kinetic studies with the non-nucleoside human immunodeficiency virus type-1 reverse transcriptase inhibitor U-90152E. *Biochemical Pharmacology* **47**:2017–2028 (1994).
2. M. S. Bergren, R. S. Chao, P. A. Meulman, R. W. Sarver, M. A. Lyster, J. L. Havens, and M. Hawley. Solid phase diversity of delavirdine mesylate. *J. Pharm. Sci.* **85**:830–837 (1996).
3. H. Martinez, S. R. Byrn, and R. R. Pfeiffer. Solid state chemistry and crystal structure of cefactlor dihydrate. *Pharm. Res.* **7**:147–153 (1990).
4. S. R. Byrn, P. A. Sutton, B. Tobias, J. Frye, and P. Main. The crystal structure, solid-state NMR spectra and oxygen reactivity of five crystal forms of prednisolone tert-butylacetate. *J.A.C.S.* **110**:1609–1614 (1988).
5. G. A. Jeffrey, R. A. Wood, P. E. Pfeffer, and K. B. Hicks. Crystal structure and solid-state NMR analysis of lactulose. *J.A.C.S.* **105**:2128–2133 (1983).
6. R. K. Harris, A. M. Kenwright, B. J. Say, and R. R. Yeung. Cross-polarization/magic angle spinning NMR studies of polymorphism: cortisone acetate. *Spectrochim. Acta.* **46A**:927–935 (1990).
7. R. A. Fletton, R. W. Lancaster, R. K. Harris, K. J. Packer, D. N. Waters, and A. Yeadon. A comparative spectroscopic investigation of two polymorphs of 4′-methyl-2′-nitroacetanilide using solid-state infrared and high resolution solid-state nuclear magnetic resonance spectroscopy. *J. Chem. Soc. Perkin. Trans. II* 1705–1709 (1986).
8. N. J. Clayden, C. M. Dobson, L. Y. Lian, and J. M. Twyman. A solid-state 13C nuclear magnetic resonance study of the conformational states of penicillins. *J. Chem. Soc. Perkin. Trans. II* 1933–1940 (1986).
9. D. L. VanderHart. Influence of molecular packing on solid-state

^{13}C chemical shifts. The n-alkanes. *J. Mag. Res.* **44**:117–125 (1981).
10. L. E. Diaz, F. Morin, C. L. Mayne, D. M. Grant, and C. Chang. Conformational analysis of DL-, L-, and D- methionine by solid-state ^{13}C NMR spectroscopy. *Mag. Res. Chem.* **24**:167–170 (1986).
11. F. G. Morin, W. J. Horton, D. M. Grant, D. K. Dalling, and R. J. Pugmire. Carbon-13 magnetic resonance of hydroaromatics. 2. Conformation of tetralin and tetrahydroanthracene and their methyl derivations. *J.A.C.S.* **105**:3992–3998 (1983).
12. D. K. Dalling, K. W. Zilm, D. M. Grant, W. A. Heeschan, W. J. Horton, and R. J. Pugmire. A solution and solid carbon-13 magnetic resonance study of the conformation of 9,10-dihydronthracene and methylated derivatives. *J.A.C.S.* **103**:4817–4824 (1981).
13. C. E. Brown, S. C. Roerig, V. T. Burger, R. B. Cody, Jr., and J. M. Fujimoto. Analgesic potencies of morphine 3- and 6-sulfates after intracerebroventricular administration in mice: Relationship to structural characterization defined by mass spectrometry and nuclear magnetic resonance. *J. Pharm. Sci.* **74**:821–824 (1985).
14. M. Bardet, A. Rousseau, and M. Vincedon. High resolution solid-state ^{13}C CP/MAS NMR study of scleroglucan hydration. *Mag. Res. Chem.* **5**:886–892 (1993).
15. M. H. Frey and S. J. Opella. Observation of conformationally distinct proline residues in two cyclic peptides by solid-state nuclear magnetic resonance. *J.A.C.S.* **103**:467–468 (1981).
16. P. Gao. Determination of the composition of delavirdine mesylate polymorph and pseudopolymorph mixtures using ^{13}C CP/MAS NMR. *Pharm. Res.* **13**:1095–1104 (1996).
17. C. A. Fyfe. *Solid State NMR for Chemists*. CFC Press, Guelph, Canada, 1983. Chapter 8.
18. X. Wu and K. W. Zilm. Complete spectral editing CPMAS NMR. *J. Mag. Res. A.* **102**:205–213 (1993).
19. J. S. Fyre and G. E. Maciel. Setting the magic angle using a quadrupolar nuclide. *J. Mag. Res.* **48**:125–131 (1982).
20. L. W. Jelinski and M. T. Melchior. High-resolution NMR of solids. in C. Dybowski and R. L. Lichter (eds.), *NMR Spectroscopy Techniques*. Marcel Dekker, Inc., New York, 1985.
21. K. A. Farley, G. S. Walker, R. H. Robins, J. E. Kupstas-Guido, W. K. Dulholke, D. L. Romero, R. A. Morge, P. A. Meulman, R. S. Chao, J. L. Havens, J. R. Gage, M. A. Lyster, P. E. Fagerness, and G. E. Martin. Spectroscopic studies of delavirdine mesylate (U-90152T) a bis(heteroary)piperazine (BHAP) HIV reverse transcriptase inhibitor. *J. Heterocyclic. Chem.* **33**:493–497 (1996).
22. J. L. Koenig. *Spectroscopy of Polymers*. ACS, Washington D.C., 1992. pg 267–277.
23. A. Naito, S. Ganapathy, K. Akasaka, and C. A. McDowell. Spin-lattice relaxation of ^{13}C in solid aminoacids using the CP/MAS technique. *J. Mag. Res.* **54**:226–235–5856 (1983).
24. R. K. Harris. *Nuclear Magnetic Resonance Spectroscopy*. Pitman Publishing, Inc., Marshfield, MA, 1983. Chapter 6.